Case study

Analysis of internal corrosion in subsea oil pipeline

M.N. Ilman *, Kusmono

Department of Mechanical and Industrial Engineering, Gadjah Mada University, Jl. Grafika No. 2, Yogyakarta 55281, Indonesia

ARTICLE INFO

ABSTRACT

Failure of a subsea crude oil API 5L X52 steel pipeline which led to oil leakage has been reported to occur after 27 years in service. Some leaks were found to form at the bottom of the horizontal API 5L X52 steel pipeline near an elbow section which connected the pipeline to a riser. The present investigation aims to analyze the main cause of failure by conducting standard failure analysis methods including visual examination, chemical and mechanical characterizations, metallurgical examinations using optical microscopy in combination with scanning electron microscopy (SEM) equipped with energy dispersive X-ray (EDX) analysis and corrosion test using a three-electrode potential technique. Results of this investigation suggest that the cause of failure is electrochemical corrosion combined with mechanical process known as flow-induced corrosion. The failure mechanism is discussed with specific attentions are paid to fluid flow rate and chloride-containing water phase.

© 2013 The Authors. Published by Elsevier Ltd. Open access under CC BY-NC-ND license.

1. Introduction

Pipeline plays an important role in oil and gas industries. Up to now pipeline is perhaps the most economical and efficient means of large scale fluid transportation for crude oil and natural gas compared to rail, truck and tanker transportation in term of the flexibility of routes and large quantities to be moved on. Pipeline is commonly made of carbon steels due to some reasons, i.e. carbon steels have good mechanical properties, low cost and wider availability despite their corrosion resistance is relatively low [1]. Normally, as an oil well ages, the production of oil starts to decline whereas water and gas flow rates tend to increase. The presence of high corrosive agents such as CO_2, H_2S and chlorine compounds which are dissolved in the fluids can accelerate corrosion process inside the pipeline [2,3]. Therefore, the impact of changes in fluid composition on a pipeline should be anticipated during maintenance program.

Recently, oil leaks have been reported to occur at a horizontal crude oil subsea pipeline after 27 years in service. A schematic diagram of the crude oil flow and the actual picture of the failed crude oil pipeline under investigation are shown in Fig. 1. During operation, crude oil was pumped from subsea wells into the horizontal pipeline. The crude oil then flowed out the pipeline directly into a long radius elbow section which turned the crude oil flow vertically allowing the flow to pass through a riser for further processing in platform.

Some oil leaks were observed at the bottom of the horizontal pipeline just before the flow entered the elbow section. No other areas of damage were identified during inspection. Details of the failed pipeline and its operating data are as follows.

* Corresponding author. Tel.: +62 274 521673; fax: +62 274 521673.
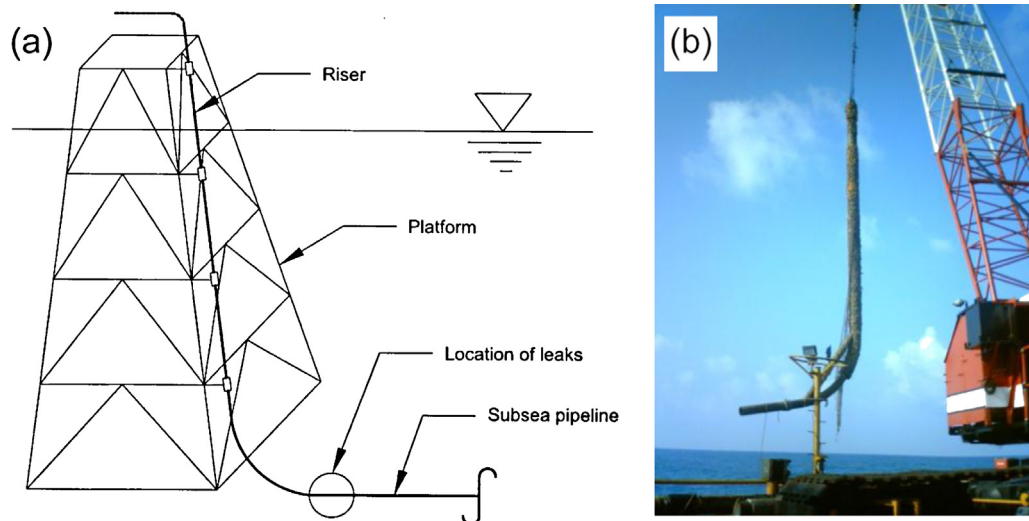 *E-mail address:* ilman_noer@ugm.ac.id (M.N. Ilman).

Fig. 1. (a) A schematic diagram of subsea pipeline-riser configuration, (b) a view of the failed subsea pipeline.

Specification and operating data	Value
Pipe outside diameter	16 in.
Length	10,677 ft
Wall thickness	0.5 in.
Material	API 5L X52
Design pressure	1480 psi
Test pressure	2225 psi
Operating pressure	170 psi (incoming) and 130 psi (outcoming)
Operating temperature	152 F (incoming)
Production (crude oil + water + gas)	2576 bopd (barrel oil per day), 28.345 bwpd (barrel water per day) and 0.441 mmscf gas per day

2. Analytical techniques

2.1. Visual examination

Fig. 2 shows visual examination results of leaks found in the pipeline. As is seen, the leaks were mainly observed at the inner surface of the pipeline. These leaks were nucleated locally at the bottom of pipeline (6 o'clock position) in the form of teardrop-shaped pits or grooves which elongated parallel to the fluid flow direction. This type of failure leads to hypothesis that the leaks are resulted from combined effect of electrochemical corrosion and fluid flow. However, this preliminary analysis needs to be verified by more detailed characterizations as shown later.

2.2. Analysis of crude oil pipeline material

Characterizations of the pipeline material were conducted using chemical composition analysis, microstructural examination and mechanical property tests including tensile test and hardness measurement. Table 1 shows chemical composition results obtained using emission spectrometer with the corresponding composition specified according to API 5L X52. The main alloying elements specified by API 5L X52 are C, Mn, Nb and V with impurities of P and S. Referring to Table 1, it can be seen that the pipeline composition fulfills that specified by API 5L X52. Of note is that elements such as Nb and V are normally added to steels as grain refiners during thermomechanical control process (TMCP).

Fig. 3 shows an optical photomicrograph of the pipeline under study. It can be seen that microstructure of the pipeline is composed of ferrite and pearlite as commonly seen in low carbon steels. These fine grained ferrite and pearlite are elongated along rolling direction known as texture. Such microstructure can give high strength in steels via grain refinement according to Hall–Petch relationship and good impact toughness to meet stringent requirements of pipeline material.
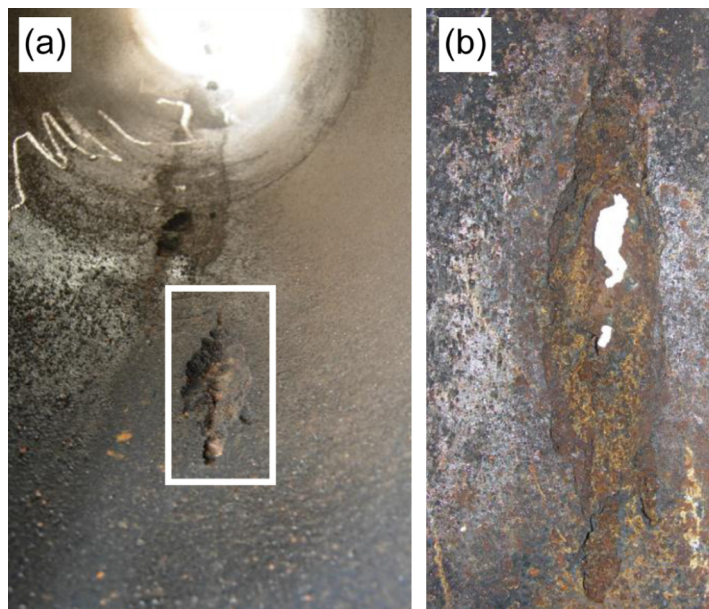
Fig. 2. (a) Leaks found at the inner surface of pipeline at 6 o'clock position, (b) magnified area outlined by square in (a).

Table 1
Chemical compositions of pipelines under study (wt%).

Material	C	Mn	Si	P	S	Al	Nb	V	Ni	Cr	Ti	Mo	Cu
Pipeline	0.166	0.608	0.262	0.094	0.024	0.042	0.022	0.010	0.066	0.045	0.007	0.062	0.133
API 5L X52	0.29 max	1.25 max	0.35 max	0.04 max	0.05 max	0.04	0.05	0.07	–	–	–	–	–

Results of tensile and hardness tests are shown in Table 2. The yield and ultimate stresses of the pipeline are 381.5 and 486.8 MPa, respectively, and these data fulfill the minimum stresses specified by API 5L X52 standard. Again, the hardness value of the pipeline does not exceed the maximum hardness specified by API 5L X52 standard. Based on the results of chemical composition, microstructural examination and mechanical property tests, it is concluded that the pipeline material is closely match to API 5L X52 carbon steel.

2.3. Analysis of water phase present in crude oil

Chemical composition of the water phase present in the crude oil was determined by atomic adsorption method with the results are given in Table 3. The main ions detected were chloride (Cl^-), bicarbonate (HCO_3^-) and sulphate (SO_4^{2-}) where chloride (Cl^-) has been known as aggressive ion. Water was identified to have pH of 8.5 or basic condition.
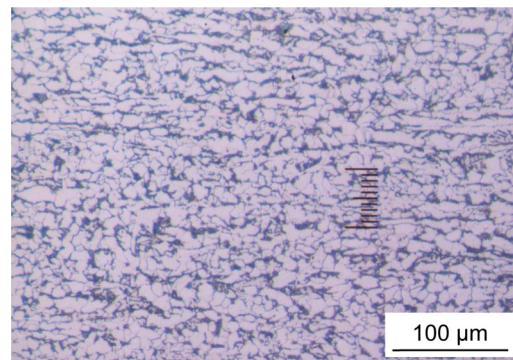

100 μm

Fig. 3. Microstructure of the pipeline under investigation.

Table 2
Mechanical properties of pipelines under study.

Material	Yield stress (MPa)	Ultimate stress (MPa)	Hardness (VHN)
Pipeline	381.5	486.8	162.3
API 5L X52	358 min	455 min	230 max

Table 3
Chemical composition of water.

Parameter	Unit	Value
pH	–	8.5
Chloride (Cl^-)	ppm	7183
Sulphate (SO_4^{2-})	ppm	324
Bicarbonate (HCO_3^-)	ppm	279

2.4. Fractography and chemical analysis of inner-side corrosion deposits

Fig. 4 shows a surface profile taken from longitudinal section of the teardrop-shaped pits. Based on the surface profile, it seemed that the crude oil flow produced undercutting in the downstream direction probably due to the presence of turbulence. The interpreted turbulent eddy is indicated by an arrow in Fig. 4.

Results of SEM microanalysis on the corroded surface near corrosion pits are shown in Fig. 5a with the EDX-spectra are shown in Fig. 5b–d. It can be seen that the region marked A in Fig. 5a is the inner layer of corrosion product where this layer is directly in contact with the steel pipeline surface. EDX-microanalysis taken from this region reveals elements such as Fe, O, C, Cl with low levels of Na, Mg, Si and S (Fig. 5b) suggesting that this inner layer is in the form of FeOCl as a result of chloride attack on hydrated passive film (FeOOH). Region marked B in Fig. 5a seems to be intermediate layer and it is composed of mainly Fe and O with a considerable amount of S as shown in Fig. 5c. At outer deposit, i.e. the region marked C in Fig. 5a, oxygen easily comes into contact with the deposit and as expected, this deposit consists of mainly Fe and O (Fig. 5d), probably in the form of hydrous ferrous oxide $Fe_2O_3 \cdot nH_2O$ or ferrous hydroxide $FeO(OH)_2$.

It seems that the chemistry of oxides change from metal-rich to oxygen-rich as the distance moves from metal-oxide interface (Fig. 5b) to outer deposits (Fig. 5c and d). These various corrosion products are consistent with the works reported by some researchers [4,5]. Of note is that C present in corrosion products probably comes from hydrocarbon and/or bicarbonate (HCO_3^-) whereas Cl is resulted from chloride ions (Cl^-) dissolved in water. The presence of S in corrosion deposits is likely associated with SO_4^{2-} in the water. Sulfate, SO_4^{2-} is anionic sulfur species in which S is fully oxidized state with the oxidation number of +6 and it is relatively unreactive.

2.5. Corrosion rate and passivity of the steel pipeline

Corrosion rate of the steel pipeline was measured using a three-electrode cell with saturated calomel electrode (SCE) as the reference electrode. To simulate actual corrosion process, the water phase extracted from crude oil was used as the electrolyte. This water was chemically identified to have 7183 ppm chloride with pH of 8.5 (basic) whereas H_2S was not detected.

Fig. 6 shows polarization diagram (Tafel plot) for the pipeline from which the corrosion rate, given in steady state current density i_{corr} ($\mu A/cm^2$), can be determined. In engineering practice, corrosion rate (r) expressed in the form of penetration per
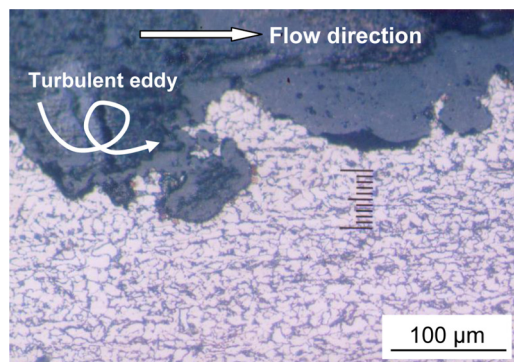

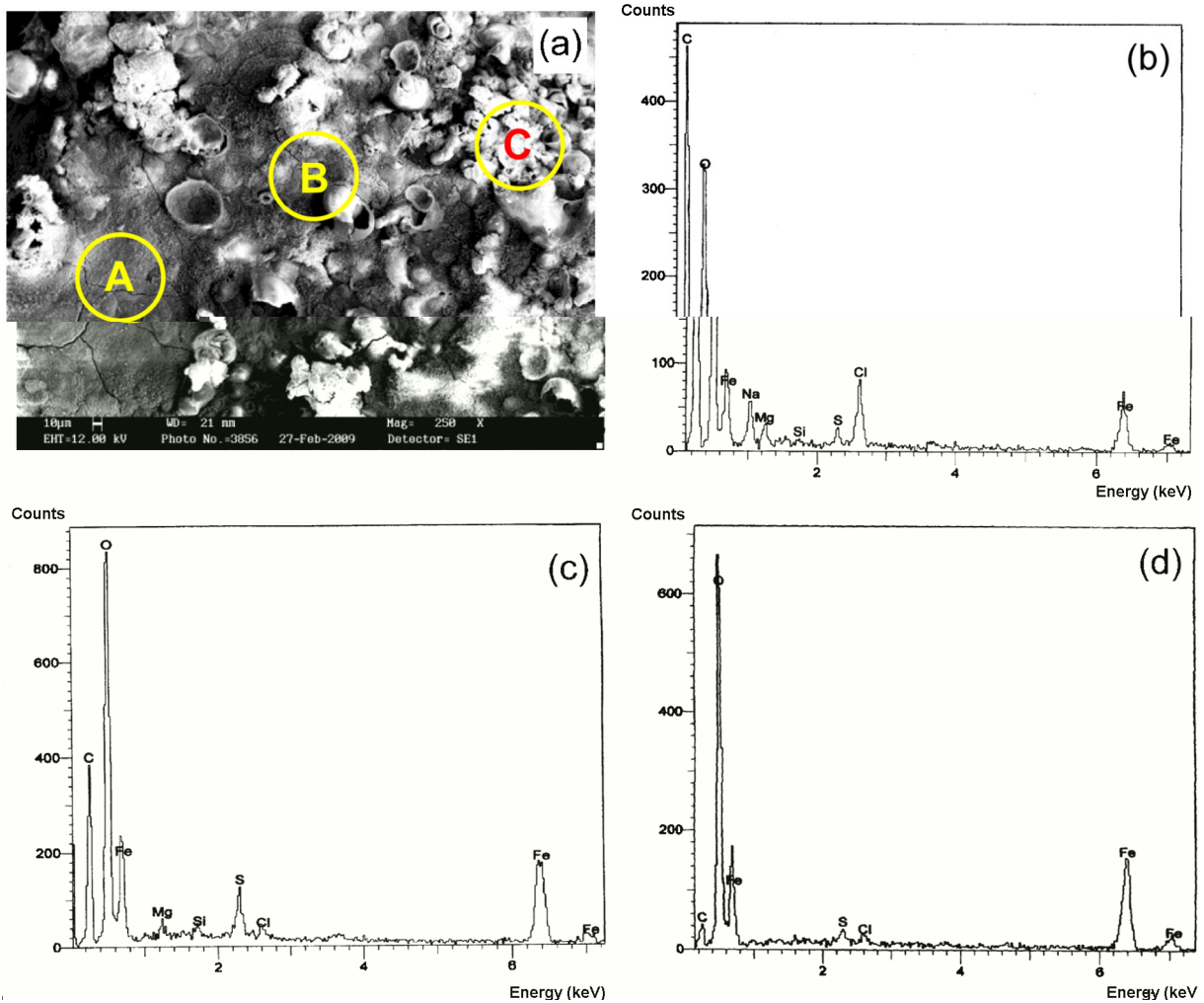**Fig. 4.** Surface profile of the pipeline along the flow direction.

Fig. 5. (a) Corrosion products at the region near leaks. (b–d) EDX-spectra taken from regions marked A–C, respectively, in (a).

unit time (mpy and mm/year) is commonly used and the corrosion rate can be calculated by substituting i_{corr}, taken from Tafel plot, to the following equations [6]:

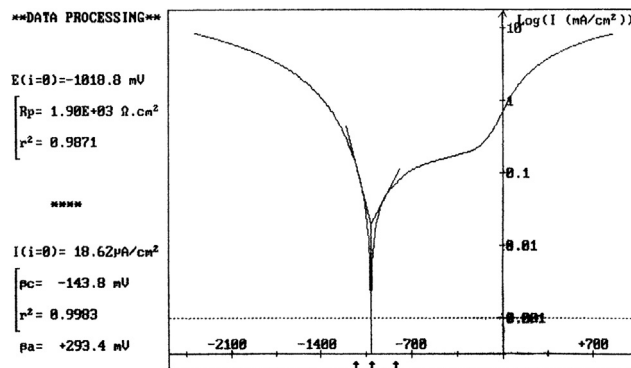$$r = 0.129 \frac{ai}{nD} = 0.129 \frac{i(EW)}{D} \quad \text{(in mpy)} \tag{1}$$

Fig. 6. Tafel plot for the pipeline in the water phase extracted from the crude oil.

or

$$r = 0.00327 \frac{ai}{nD} = 0.00327 \frac{i(EW)}{D} \quad \text{(in mm/year)} \tag{2}$$

where D is density (g/cm^3), i is current density (μA/cm^2), a is atomic mass (g/mole), n is valency. The equivalent weight (EW) in Eqs. (1) and (2) can be determined by:

$$EW = (N_{EQ})^{-1} \tag{3}$$

$$N_{EQ} = \sum \left(\frac{f_i n_i}{a_i} \right) \tag{4}$$

where f is mass fraction of element in alloys. Results of corrosion rate calculation are given in Table 4. As it is demonstrated, the corrosion rate of the steel pipeline is 18.62 μA/cm^2 or equivalent to 8.616 mpy (0.2184 mm/year) suggesting that the pipeline material has a good corrosion resistance. Of note is that the corrosion rate measured in the laboratory test would not be the same as that obtained from on-site observation due to the facts that in the laboratory test, the surface of corrosion specimen was polished with no fluid flow during the test and test temperature was lower than the actual operating temperature. However, from the view point of passivity behavior, the polarization test may give useful information on active-passive behavior of steel pipeline in aqueous environment.

Referring to Fig. 6, it can be seen that at the potential range of -700 to -175 mV SCE, the pipeline exhibits passivity presumably due to the formation of passive film [6,7].

$$Fe + H_2O + 1/2O_2 \rightarrow Fe(OH)_2 \, (\text{passivefilm}) \tag{5}$$

Breakdown of passivity starts to occur at the potential of -175 mV SCE or higher suggesting that the steel pipeline has susceptibility to pitting corrosion. This type of corrosion could be linked to aggressive agents such as chloride which destroy the passive film locally and catalyze the liberation of Fe^{3+} according to [8]:

$$FeOOH \, (\text{hydratedpassivefilm}) + Cl^- \rightarrow FeOCl + OH^- \tag{6}$$

$$FeOCl + H_2O \rightarrow Fe^{3+} + Cl^- + 2OH^- \tag{7}$$

The presence of Cl in corrosion product as shown in EDX-spectra in Fig. 5b suggests that the mechanism in which chloride ions destroy passive film is operative.

2.6. Flow pattern analysis

The analysis of flow pattern in the present investigation is based on multiphase flow consisting of crude oil, water and gas phases in horizontal pipeline. Due to density difference between liquids (crude oil and water) and gas, different flow patterns or flow regimes can occur when liquids and gas flow simultaneously inside the pipeline. Flow parameters in the forms of superficial liquid and gas velocities can be determined using the equations [9]:

$$U_{sl} = \frac{Q_l}{A_f} \tag{8}$$

$$U_{sg} = \frac{Q_g}{A_f} \tag{9}$$

where U_{sl} and U_{sg} are superficial liquid velocity and superficial gas velocity, respectively, Q_l and Q_g are liquid and gas volumetric flow rates, respectively, and A_f is pipeline flow cross-sectional area. By using flow rate data in Section 1 above and converting the data into SI unit, the flow regimes can be determined using Eqs. (8) and (9) as follows:

Referring to Table 5, it can be seen that U_{sl} and U_{sg} are relatively low and based on gas–liquid flow regime curve for horizontal pipeline [9], the flow pattern is expected to take place in the form of stratified flow where the gas and liquid

Table 4
Corrosion rates of pipelines under study.

Material	i_{corr} (μA/cm^2)	N_{EQ}	EW	D (g/cm^3)	Corrosion rate	
					mpy	mm/year
Pipeline	18.62	0.03630	27.55	7.68	8.616	0.2184

Table 5
Calculation results of U_{sl} and U_{sg} with expected flow pattern.

Liquid flow rate (Q_l) (m³/s)	Gas flow rate (Q_g) (m³/s)	Liquid velocity (U_{sl}) (m/s)	Gas velocity (U_{sg}) (m/s)	Flow pattern
4.7918×10^{-3}	0.1445	0.0420	1.2675	Stratified flow
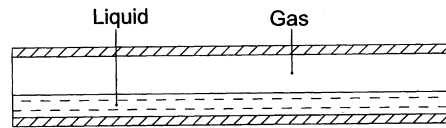
Fig. 7. Gas–liquid stratified flow in horizontal pipeline.

completely segregate from each other as shown in Fig. 7. In such a case as this, water preferentially forms at the bottom of the pipeline allowing the pipe surface to come into contact with water phase.

3. Discussion

Based on visual analysis, it can be seen that the leaks are in the form of teardrop shaped pits or grooves at the bottom of the pipeline (6 o'clock position) where water layers preferentially form. The absence of scales or deposits around the grooves suggest that the pipeline is locally attacked by flow-induced corrosion. Such corrosion initially produces brittle scales or rusts on the pipe surface exposed to the fluid. These scales act as barrier between the metal surface and the fluid so that further corrosion penetration is inhibited. Subsequently, the fluid flow causes the erosion process and the scales or corrosion products are periodically scoured from the exposed surface hence increasing corrosion rate along the flow direction.

Failure mechanism of the horizontal subsea pipeline due to flow-induced corrosion is described in Fig. 8. According to the flow analysis as previously discussed, the flow pattern is expected to take place in the form of stratified flow where the gas and liquid completely segregate from each other and the water layer is present at the bottom of the oil pipeline. As the crude oil flows through the elbow section, the flow must turn resulting in impacts on the regions near the bend pipeline wall. This impact combined with chloride in the crude oil, the eddy current and possibly entrainment of sand in the pipeline have a potency to destroy the protective film. Once the protective film is destroyed, the pipeline surface is exposed to water and oxidation-reduction reactions are expected to occur.

The steel surface will act as anode and it dissociates as positively charged ions leaving electrons behind.

$$Fe \rightarrow Fe^{2+} + 2e^- \tag{10}$$

In neutral and basic condition, oxygen present in the water subsequently consumes the electrons from anode according to the following reaction.

$$H_2O + 1/2O_2 + 2e^- \rightarrow 2OH^- \tag{11}$$

The addition of the two half-reactions leads to the overall reactions as follow:

$$Fe + H_2O + 1/2O_2 \rightarrow Fe(OH)_2 \tag{12}$$
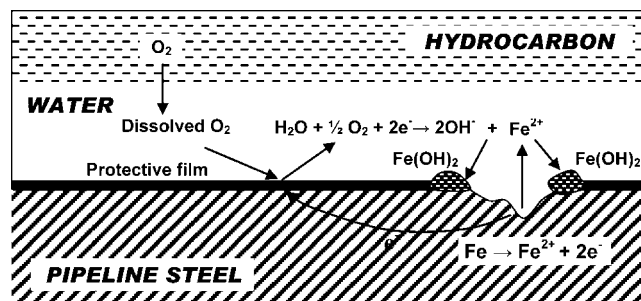
Fig. 8. Proposed mechanism of flow induced corrosion in oil pipelines.

The corrosion product of ferrous hydroxide [$Fe(OH)_2$] forms a diffusion-barrier layer around the pit mouth through which oxygen must diffuse. At the outer surface of the $Fe(OH)_2$ layer, access to dissolved oxygen is easy leading to the formation of ferric hydroxide, in accord with

$$2Fe(OH)_2 + H_2O + 1/2O_2 \rightarrow 2Fe(OH)_3 \tag{13}$$

Ferric hydroxide [$Fe(OH)_3$] appears to be reddish-brown in color as shown in Fig. 2b. It seems that the $Fe(OH)_2$ or $Fe(OH)_3$ deposits resulted from corrosion reaction are then scoured from the exposed surface by the fluid flow hence increasing corrosion rate along the flow direction. As a result, the corrosion rate at the spread of corrosion downstream is higher than that of penetration and sideways. Such corrosion attack changes from pinhole shape, typical of purely corrosive attack to become teardrop-shaped pits or grooves.

4. Conclusions and recommendations

1. Flow induced corrosion seems to be the main cause of leakages that occur locally at the horizontal subsea pipeline near an elbow section.
2. Combined effect of pitting corrosion and erosive flow increases corrosion rate along the flow direction resulting in teardrop-shaped pits.
3. The damage prevention options are suggested: first, prevent water separation by increasing oil flow sufficiently so that the pipeline surfaces are maintained oil wetted and secondly, give inhibitor injection into an oil pipeline fluid stream.

Acknowledgement

References

[1] Tawancy HM, Al-Hadhrami LM, Al-Yousef FK. Analysis of corroded elbow section of carbon steel piping system of oil-gas separator vessel. Case Studies in Engineering Failure Analysis 2013;1:6–14.
[2] Rodriguez MALH, Delgado DM, Gonzalez R, Unzueta AP, Solis RDM, Rodriguez J. Corrosive wear failure analysis in a natural gas pipeline. Wear 2007;263:567–71.
[3] Palmer AC, King RA. Subsea pipeline engineering. Oklahoma: PennWell; 2004.
[4] Azevedo CRF. Failure analysis of a crude oil pipeline. Engineering Failure Analysis 2007;14:978–94.
[5] Waanders FB, Vorster SW. Corrosion products formed on mild steel samples submerged in various aqueous solution. Hyperfine Interactions 2002;139:239–44.
[6] Jones DA. Principles and prevention of corrosion. New York: Prentice-Hall Inc.; 1996.
[7] Uhlig HH, Revie RW. Corrosion and corrosion control. New York: John Willey & Sons; 1995.
[8] Jones DA. In: Parkins, editor. Corrosion processes. NewYork: Applied Science; 1982.
[9] Guo B, Song S, Chacko J, Ghalambor A. Offshore pipelines. Burlington: Gulf Professional Publishing; 2005.